Interaction of Eu-isotopes with saponite as a component of the engineered barrier

María D. Alba (a), Miguel A. Castro (a), P. Chaín (a), Santiago Hurtado (b), M. Mar Orta (a), M. Carolina Pazos (a), María Villa (b)

a Instituto Ciencia de los Materiales de Sevilla, CSIC-US, Avda. Americo Vespucio, 49, 41092 Sevilla, Spain

b Centro de Investigación, Tecnología e Innovación de la Universidad de Sevilla, CITIUS, Avda. Reina Mercedes, 4, 41012 Sevilla, Spain

Abstract

Bentonite is accepted as the best clay material in the engineered barrier of deep geological repositories (DGRs) for radioactive waste disposal. In recent years, the interactions between a wide range of rare-earth (REE) cations and smectites have been studied. A combined study of stable europium and radioactive isotopes is reported here. Saponite was subjected to hydrothermal reactions with stable and radioactive (152Eu) europium ions under subcritical conditions. The structural changes of saponite were evaluated by XRD and SEM. The effect of temperature and reaction time on the changes was quantified by measuring 152Eu through gamma spectrometry. The reaction between europium and saponite was a first-order reaction. The presence of Eu in the precipitate in an amount much higher than the cation exchange capacity of saponite confirmed participation of chemical reactions or surface adsorption in the europium immobilization, even at temperatures as low as 150 °C. The reaction rate constant indicated that an 8- to 9-month period was needed for the completion, without significant changes, of the europium/saponite chemical reaction under the subcritical conditions of 200 °C and 350 °C.

Keywords

Engineering barrier; Radionuclide; Bentonite

1. Introduction

The management of radioactive waste containing actinides is currently a key environmental problem due to the need for its long-term, safe and efficient storage. The deep geological repository (DGR) concept involves the placement of long-living high-activity radioactive waste (HARW) in rooms excavated deep within a stable, low-permeability bedrock. In many countries, the DGRs are based on a passive multi-barrier system approach that combines waste packages, engineered seals, and bedrock whereby the major responsibility for safety falls on the engineered barrier system (EBS). Nowadays, bentonite is accepted as the best clay material for the engineered barrier of DGRs (Bailey, 1980). In almost all repositories of this type it is assumed that the geosphere surrounding the EBS is saturated with water since

groundwater gradually seeps back into the tunnel and could be in contact with the EBS. Under saturation conditions, bentonite, due to its high content of smectite, swells and seals the tunnel, restricting almost all flow of water inside the EBS (Bailey, 1980).

The interaction of 4f elements, such as La, Lu, Nd and Sm, with natural and synthetic clay minerals during thermal and hydrothermal reactions was studied in a systematic and fundamental way (Alba and Chain, 2005, Alba and Chain, 2007, Alba et al., 2009a and Alba et al., 2009b). A never studied reaction mechanism, based on the interaction between the lanthanide cations and the clay mineral, was identified (Trillo et al., 1994). Under subcritical temperature and pressure conditions (374.3 °C, 218 atm), an interaction between smectites and rare-earth elements (REE) was found to exist (Chapman and Smellie, 1986) and an insoluble disilicate, REE2Si2O7, was generated (Becerro et al., 2003). The reaction extends to the whole set of smectites, although their reactivity differs, with saponite as the most reactive (Alba et al., 2001). These results implied an efficient mechanism of the engineered barrier (bentonite barrier) for highly active radioactive waste (HARW) management when the properties of bentonites (cation exchange and swelling capacity), that are responsible for the physical retention, fail this retention.

These systematic studies were performed by using lanthanide ions as the HARW chemical analogous. If uranium (95% of the spent fuel) were disregarded, an average composition of the spent-fuel pellets of reference would be approx. 18 mass% of plutonium and 2 mass% of equally distributed neptunium and americium, with the remaining actinides as minor elements (Astudillo, 2001). Therefore, the feasibility of the chemical-interaction immobilization mechanism for the main HARW present in the nuclear waste remains to be tested.

Thus, in order to understand the above-mentioned hydrothermal reaction, a combined study was performed: On one hand, the structural changes of saponite by the stable isotopes should be considered. On the other hand, together with a stable isotope, a radioisotope can be added in ultra-trace concentrations, which makes it possible to quantitatively determine the distribution of the REE cations between the solid and the liquid parts of the reaction.

Many studies in the literature are dedicated to the adsorption of the stable europium ions by clay minerals. The cation exchange process is the main adsorption mechanism at 25 °C–150 °C and at atmospheric pressure (Sánchez et al., 2006 and Tertre et al., 2006). The study of the behavior of radioisotopes in various matrices is widespread, for example adsorption and desorption properties in contaminated soils have been studied in Liu et al. (2003) and in Spalding (2001), while soil-to-plant transfer properties have been investigated by Rigol et al. (2008). Studies of the adsorption of radioisotopes on clay minerals include those by Devivier et al. (2004) for 125I, Vejsada et al. (2005) for 134Cs, and Rabung et al. (2005) for trace concentrations of curium. The behavior of europium ions in clay minerals has been widely studied, for example, adsorption studies have been carried out by Rabung et al. (2005), and in Fan et al. (2009), whereas Rahman et al. (2007) focused on leaching studies.

Depending on the temperature, REE2Si2O7 is formed, under hydrothermal conditions at 300 °C, from a wide set of REE3+ cations, such as Sc3+, Y3+, La3+, Nd3+, Sm3+ and Lu3+, (Alba et

al., 2009a). In order to evaluate the applicability of the long immobilization process in real repositories, it is necessary to explore the feasibility of the reaction below 200 °C. The study of structural changes below this temperature, however, is not always achievable (Allen and Wood, 1988, Mather et al., 1982 and Savage and Chapman, 1982), and therefore higher temperatures are taken as appropriate conditions for the simulation of deep geological disposal conditions and for an increase of the reaction rates.

The use of stable isotopes enables an analysis to be carried out of the structural changes of the bentonite after the hydrothermal reaction with REE. The use of radioactive isotopes enables to obtain further data: a) the immobilization capacity can be quantitatively determined; b) the kinetics of the process can be analyzed; c) the proposed reaction mechanism can be tested in a wide range of temperatures, even when the extent of the reaction is insufficient to enable detection of structural changes; and d) an appropriate methodology can be established to extend the study of instable radionuclides.

Eu3+ seems to be the most suitable REE cation for this study since its physical properties (cation size, hydrolization constant, and oxidation state) are comparable with those of Am3+ and Cm3+ (Bradbury et al., 2005 and Fan et al., 2009). It is available as stable isotopes, 151Eu, 153Eu, and the radioactive isotope, 152Eu (T1/2 = 13.5 years). Therefore, in this experimental study we address the rate and mechanism of Eu3+ ion as a model system, under conditions similar to those predicted for the nuclear waste storage assessment. In geochemical processes of waste degradation and waste/rock interaction, the expected temperatures reach up to approx. 200 °C (Savage and Chapman, 1982). However, many studies devoted to simulating deep geological disposal conditions used temperatures of up to 350 °C to increase the reaction rates, (Allen and Wood, 1988, Mather et al., 1982 and Savage and Chapman, 1982).

2. Experimental

2.1. Saponite

Saponite was obtained from the Source Clay Minerals Repository University of Missouri (Columbia) and had the following chemical formula: Na0.61K0.02Ca0.09 (Si7.2Al0.8)IV(Mg5.79 Fe2+0.15)VIO20(OH)4 (Alba et al., 2001). The interlayer cation concentration and the water content were estimated to be 103.0 meq/100 g and 9.2 mass% (Chain, 2007).

2.2. Eu3+ solution

Two sets of starting solutions of 7.9 · 10− 2 M Eu(NO3)3 (151Eu and 153Eu, with 52.2% 153Eu) were prepared: i) The first solution contained purely stable Eu isotopes and ii) the second solution was enriched with the radioisotope 152Eu. A volume of 1 ml from a diluted standard solution (9.8 Bq/ml) up to a total activity of 9.8 Bq was added to 35 ml of the former solution, i.e. a compromise between low radioactivity concentrations for safe handling and high counting rates to get fast measurements. Due to its short half-life (13.5 years) 10− 14 mol of 152Eu were added.

The pH of both solutions was adjusted to pH = 6.0–6.5, by slowly adding 0.05 M ammonia solution under stirring.

2.3. Hydrothermal reactions

300 mg of the powdered samples were dispersed in 40 ml of the Eu3+ solutions and were heated in a stainless steel reactor, (Perdigón, 2002), at the temperatures and times summarized in Table 1. The cells marked with vertical line correspond to the treatment with a starting solution of 7.9 · 10− 2 M Eu(NO3)3, the gray color cells with a starting solution of 7.9 · 10− 2 M Eu(NO3)3 enriched with the 152Eu isotope. The reaction products were collected by filtering, washed with distilled water, and dried in air at 60 °C. The reaction solution and the washing liquid were kept for the quantitative analysis of europium by gamma spectroscopy.

For the evaluation of possible artifacts such as adsorption onto the wall of the reactor, the reactor vessel with 40 ml of Eu(NO3)3 7.9 · 10− 2 M was heated at 350 °C for 4.5 days. The 152Eu content of the remnant solution showed that the Eu adsorption onto the container was negligible under these reaction conditions.

2.4. Characterization methods

X-ray powder diffraction (XRD) patterns were obtained with a Bruker D8I instrument, at the CITIUS, University of Seville (Spain) (a Ni-filtered Cu Kα radiation, 40 kV, 40 mA, scan steps of 0.05° 2θ, with a counting time of 3 s). The crystalline phases were identified by using the computer program X'Pert HighScore (Philips Analytical B.V. Almelo, The Netherlands).

Scanning electron microscopy (SEM) was used to observe the materials of which no appreciable crystalline phases were observed by XRD. The morphology and chemical compositions of the samples were analyzed, at the Microscopy Service of CITIUS, University of Seville (Spain), in a scanning electron microscope (JEOL 6460LV) equipped with EDX.

The radioactive europium, 152Eu, was measured with an HPGe coaxial gamma detector, at the CITIUS, University of Seville (Spain). To calibrate the counting efficiency, 152Eu-free, solid samples obtained after the hydrothermal reaction were spiked with a known amount of 152Eu. The activity concentration of 152Eu was measured in the liquid and solid phases.

3. Results and discussion

3.1. Structural studies

The XRD patterns of the saponite and those after reaction with 7.9 · 10− 2 M Eu(NO3)3 at 350 °C, 200 °C and 150 °C, are displayed in Fig. 1. The pattern of the original saponite (Fig. 1a) showed the general and basal reflections. The hk bands were composed of asymmetrical reflections with the characteristic “saw-tooth” shape of the two-dimensional reflections (Warren, 1941). The basal reflections were symmetrical. The 12.30 Å d001 value of unreacted saponite corresponded to the monolayer hydrate of Na-saponite (Alba et al., 2001, Grim, 1968, Ravina and Low, 1977 and Warren, 1941).

After the hydrothermal reaction at 150 °C for 47 days, (Fig. 1b) the basal spacing of saponite was increased to 14.30 Å, in agreement with data reported for smectites saturated with

multivalent cations (Ravina and Low, 1977). Also, the position of the 060 reflection, in the range of the trioctahedral smectites (Grim, 1968), was slightly shifted to d060 = 1.526 Å. Additionally, small reflections in the 25–30° 2θ range were observed and corresponded to F-Eu2Si2O7 (PDF 87–2475, marked with F) and Eu(OH)3 (PDF 83–2305, marked with h). The XRD pattern was noisy and showed a prominent background which indicated the partial disruption of the saponite framework.

The hydrothermal reaction at 350 °C yielded similar XRD patterns (Fig. 1c and d) which were dominated by reflections of F-Eu2Si2O7 (PDF 87–2475, marked with F), crystalline Eu(OH)3 (PDF 83–2305, marked with h), Eu2O3 (PDF 34–392, marked with o) and EuONO3 (PDF 31–518, marked with n). These phases coexisted with the remnant clay mineral or a new mixed-layered clay mineral which was characterized by a set of basal reflections with d002 = 14.6 Å and the absence of the hk reflections. The only effect of the reaction time was the better crystallization of the new phases (Fig. 1c and d). Thus, temperature played a greater role than time in the formation of the disilicate, as is expected due to the laws of thermodynamics and kinetics.

The electron micrographs and the EDX analysis of the saponite reacted with Eu3+ at 150 °C for 47 days (Fig. 2) showed lamellar morphology of the majority of the particles (Fig. 2a) with some small brilliant particles on their surfaces. The EDX spectrum of this saponite (Fig. 2c) was characterized by the absence of Na+, low content of Mg2+, and a relatively high amount of Eu3+ when compared to the original saponite (Fig. 2b). When saponite was reacted at 350 °C, most of the particles again showed the lamellar morphology (Fig. 3a and b). The EDX spectra (Fig. 3d) were characterized by the Kα1 lines of Si, Al and Mg and Mα, and Lα and Lβ lines of Eu. The decrease of the Mg content and the absence of Na, in comparison with the original saponite (Fig. 3c), were due to the leaching of Mg ions from the structure and the exchange of Na+ by Eu3+ in the interlayer space. This is in line with the XRD patterns that showed a moderately degraded state of the layers and an increased basal spacing (Fig. 1c and d). The altered saponite seemed to form aggregates and showed an increasingly blocky morphology with increasing reaction time. In addition to the lamellar particles, some compact particles with brilliant appearance under the backscattering electron beam were also observed with a chemical composition (Fig. 3d) compatible with the europium crystalline phases already observed by XRD, e.g. Eu2Si2O7, Eu(OH)3, Eu2O3 or EuONO3. These brilliant particles were more abundant at the longer reaction times (Fig. 3b).

Thus, in the initial step of the reaction at 150 °C, the Na+ ions of the saponite were exchanged by Eu3+. As the reaction progressed up to 350 °C, the saponite structure was decomposed forming crystalline F-Eu2Si2O7. Other minor europium phases were also observed at 150 °C and 350 °C.

3.2. The extent of the reaction

The parameters used for the quantitative evaluation of the extent of the europium and silicate reaction as a function of time and temperature are summarized in Table 2. The amount of europium bound by saponite was calculated from the measured radioactivity in the liquid (non-reacted) and the solid (reacted) phases after the hydrothermal reaction. The content of silicon involved in the chemical immobilization mechanism indicated the progress of Eu2Si2O7 formation.

Even at the lowest temperature and reaction time, the amount of bound europium ions was more than three times the cation exchange capacity of saponite (103.0 meq/100 g). This clearly indicated that in addition to the ion exchange, europium phases were formed.

The amount of bound europium ions after the reaction for 20 days changed almost linearly with the temperature (Fig. 4): 390 ± 20 meq/100 g at 150 °C, to 990 ± 40 meq/100 g at 200 °C, and to 1170 ± 30 meq/100 g at 350 °C, where 390 and 990 are the average values obtained from two measurements. The dependence on the reaction time could not be clearly seen at 150 °C, since, at that temperature, the reaction times were too short.

The results were fitted to an exponential function where the exponent corresponded to the reaction rate constant, k. I0 was in agreement with the average 152Eu recovered in the liquid and in the solid. The fitting indicated that the reaction between europium and saponite was a first-order reaction.

$$I = I_0 e^{kt}$$

$$350^{\circ}\mathrm{C} \quad I = (5.52 \pm 0.04) e^{-(0.0133 \pm 0.0007)t} \qquad R^2 = 0.992 \quad \text{(a)}$$

$$200^{\circ}\mathrm{C} \quad I = (8.31 \pm 0.02) e^{-(0.0119 \pm 0.0001)t} \qquad R^2 = 0.999 \quad \text{(b)}$$

For 350 °C and 200 °C, the best fit was exponential but with a rate constant that slightly decreased between 350 °C and 200 °C (1.33 · 10− 2 vs 1.19 · 10− 2). The reaction was almost three times faster at 350 °C than at 200 °C. Using the calculated reaction rates, it can be inferred that the chemical immobilization of Eu ion would be completed after 8–9 months of reaction under subcritical conditions at 350 °C and at 200 °C. Since the reaction times at 150 °C were not long enough, fitting could not be carried out at this temperature.

4. Conclusions

The amount of Eu in the reacted saponite in much higher amounts than corresponding to the cation exchange capacity of saponite was the result of the cation exchange and the neoformation of the europium phases, even at temperatures as low as 150 °C. The kinetic parameters of europium immobilization were evaluated. Moreover, these results may be used to predict the behavior of HARW cations (Am, Cm, Th, U, and Pu) within the bentonite barriers when structural analysis is unfeasible.

Acknowledgments

We gratefully acknowledge financial support from Ministerio del Medio Ambiente y Medio Rural y Marino project no. 300/PC08/3-01.1 and DGICYT project no. CTQ2010-14874. Finally, we thank ENRESA for its financial support.

References

M.D. Alba, P. Chain

Interaction between lutetium cations and 2:1 aluminosilicates under hydrothermal treatment

Clays and Clay Minerals, 53 (2005), pp. 39–46

M.D. Alba, P. Chain

Persistence of lutetium disilicate

Applied Geochemistry, 22 (2007), pp. 192–201

M.D. Alba, A.I. Becerro, M.A. Castro, A.C. Perdigón

Hydrothermal reactivity of Lu-saturated smectites: part I. A long-range order study

American Mineralogist, 86 (2001), pp. 115–123

M.D. Alba, P. Chain, M.M. Orta

Chemical reactivity of argillaceous material in engineered barrier. Rare earth disilicate formation under subcritical conditions

Applied Clay Science, 43 (2009), pp. 369–375

M.D. Alba, P. Chain, M.M. Orta

Rare-earth disilicate formation under Deep Geological Repository approach conditions

Applied Clay Science, 46 (2009), pp. 63–68

C.C. Allen, M.I. Wood

Bentonite in nuclear waste disposal: a review of research in support of the basalt waste isolation project

Applied Clay Science, 3 (1988), pp. 11–30

J. Astudillo

El almacenamiento geológico profundo de los residuos radiactivos de alta actividad. Principios básicos y tecnología. Editorial ENRESA (2001)

S.W. Bailey

Structures of layer silicates

G.W. Brindley, G. Brown (Eds.), Crystal Structures of Clay Minerals and Their X-ray Identification, Mineralogical Society, London (1980), pp. 1–123

A.I. Becerro, M. Naranjo, M.D. Alba, J.M. Trillo

Structure-directing effect of phyllosilicates on the synthesis of y-Y2Si2O7. Phase transitions in Y2Si2O7

Journal of Materials Chemistry, 13 (2003), pp. 1835–1842

M.H. Bradbury, B. Baeyens, H. Geckeis, Th. Rabung

Sorption of Eu(III)/Cm(III) on Ca-montmorillonite and Na-illite. Part 2: surface complexation modeling

Geochimica et Cosmochimica Acta, 69 (2005), pp. 5403–5412

Chain, P., 2007. Síntesis Hidrotermal de Disilicatos de Tierras Raras a partir de Silicatos Laminares: Un Mecanismo Inmovilizador de Residuos Radiactivos de Alta Actividad. Ph.D. Thesis, University of Seville, Spain.

N.A. Chapman, J.A.T. Smellie

Natural analogues to the conditions around a final repository for high-level radioactive waste

Chemistry and Geology, 55 (1986), pp. 167–173

K. Devivier, I. Devol-Brown, S. Savoye

Study of iodide sorption to the argillite of Tournemire in alkaline media

Applied Clay Science, 26 (2004), pp. 171–179

Q.H. Fan, X.L. Tan, J.X. Li, X.K. Wang, W.S. Wuand, G. Montavon

Sorption of Eu(III) on attapulgite studied by batch, XPS, and EXAFS techniques

Environmental Science & Technology, 43 (2009), pp. 5776–5782

R.E. Grim

Clay Mineralogy

McGraw-Hill Book Company, New York (1968)

C. Liu, J.M. Zachara, O. Qafoku, S.C. Smith

Effect of temperature on Cs+ at the Hanford Site, U.S.A

Environmental Science & Technology, 37 (2003), pp. 2640–2645

J.D. Mather, N.A. Chapman, J.H. Black, B.C. Lintern

The geological disposal of high-level radioactive waste — a review of the Institute of Geological Sciences Research programme

Nuclear Energy, 21 (1982), pp. 167–173

Perdigón, A.C., 2002.

Estudio del sistema saponita/Lu(NO3)3/H2O en condiciones hidrotérmicas. Ph.D. Thesis, University of Seville, Spain.

Th. Rabung, M.C. Pierret, A. Bauer, H. Geckeis, M.H. Bradbury, B. Baeyens

Sorption of Eu(III)/Cm(III) on Ca-montmorillonite and Na-illite. Part 1: batch sorption and time-resolved laser fluorescence spectroscopy experiments

Geochimica et Cosmochimica Acta, 69 (2005), pp. 5393–5402

Rahman et al., 2007

R.O.A. Rahman, A.A. Zaki, A.M. El-Kamash

Modeling the long-term leaching behavior of 137Cs, 60Co and 152,154Eu radionuclides from cement–clay matrices

Journal of Hazardous Materials, 145 (2007), pp. 372–380

A. Rigol, M. Camps, A. de Juan, G. Rauret, M. Vidal

Multivariate Soft-Modeling to Predict Radiocesium Soil-to-Plant Transfer

Environmental Science Technology, 42 (2008), pp. 4029–4036

I. Ravina, P.F. Low

Change of b-dimension with swelling of montmorillonite

Clays and Clay Minerals, 25 (1977), pp. 201–204

A. Sánchez, Y. Echeverría, C.M. Sotomayor Torres, G. González, E. Benavente

Intercalation of europium (III) species onto bentonite

Materials Research Bulletin, 41 (2006), pp. 1185–1191

D. Savage, N.A. Chapman

Hydrothermal behaviour of simulated waste glass- and waste-rock interaction under repository conditions

Chemical Geology, 36 (1982), pp. 59–86

B.P. Spalding

Fixation of radionuclides in soil and minerals by heating

Environmental Science & Technology, 35 (2001), pp. 4327–4333

E. Tertre, G. Berger, E. Simoni, S. Castet, E. Giffaut, M. Loubert, H. Catalette

Europium retention onto clay minerals from 25 to 150 °C: experimental measurements, spectroscopic features and sorption modelling

Geochimica et Cosmochimica Acta, 70 (2006), pp. 4563–4578

J.M. Trillo, M.D. Alba, R. Alvero, M.A. Castro, A. Muñoz-Páez, J. Poyato

Inorganic Chemistry, 33 (1994), pp. 3861–3862

J. Vejsada, T.D. Hradil, Z. Randac, E. Jelinek, K. Stulik

Adsorption of cesium on Czech smectite-rich clays—a comparative study

Applied Clay Science, 30 (2005), pp. 53–66

B.E. Warren

X-ray diffraction by random layers

Physical Review, 59 (1941), pp. 693–698

Figure captions

Figure 1. XRD patterns of (a) the starting saponite, (b) after the hydrothermal reaction at 150 °C for 47 days, (c) 350 °C for 4.5 days, and (d) 350 °C for 9 days. F = F-Eu2Si2O7 (PDF 87–2475), n = EuONO3 (PDF 31–518), h = Eu(OH)3 (PDF 83–2305), and, o = Eu2O3 (PDF 34–392).

Figure 2. (a) Micrograph of the saponite hydrothermally reacted at 150 °C for 47 days with a solution of 7.9 · 10–2 M Eu(NO3)3; (b) EDX of the original saponite, and (c) EDX of the particles shown in a.

Figure 3. (a and b) Micrographs of the saponite hydrothermally reacted at 350 °C for 4.5 days and 9 days with a solution of 7.9 · 10− 2 M Eu(NO3)3; (c) EDX of the original saponite; (d) EDX of the lamellar particles; and (e) EDX of the brilliant particles.

Figure 4. The plot of 152Eu activity recovered in the liquid phase vs time at (a) 350 °C, (b) 200 °C and (c) 150 °C and the fitting to an exponential function.

Table 1

Temperature (°C)	Time (days) 2.2	4.5	7	9	14	20	28	47	56
350									
200									
150									

Vertical line = starting solution of $7.9 \cdot 10^{-2}$ M $Eu(NO_3)_3$.Gray colors = starting solution of $7.9 \cdot 10^{-2}$ M $Eu(NO_3)_3$ enriched with ^{152}Eu isotope.

Table 2

Table 2. ^{152}Eu activity, amount of Eu^{3+} immobilized in the solid and mol% of silicon corresponding to $Eu_2Si_2O_7$. The uncertainty corresponds to 1σ and was deduced after statistical analysis of the radioactive measurements.

Temperature (°C)	Time (Days)	^{152}Eu activity (Bq)				meq Eu^{3+}/100 g saponite				Si (mol%)	
		Liquid	± σ	Solid	± σ	% solid[a]	± σ	Solid[b]	± σ	Solid[c]	± σ
350	2.2	5.4	0.2	0.79	0.02	12.7	0.4	430	10	15.6	0.4
	4.5	5.2	0.2	1.12	0.03	17.8	0.5	610	20	21.8	0.6
	9	4.9	0.1	1.30	0.03	21.0	0.6	720	20	25.8	0.7
	20	4.25	0.1	2.21	0.05	34	1	1170	30	42	1
200	4	7.9	0.2	2.02	0.05	20.4	0.7	690	20	25.0	0.7
	9	7.5	0.1	2.63	0.05	26.0	0.6	890	20	31.9	0.7
	20	5.8	0.1	2.83	0.05	32.6	0.7	1110	20	40.0	0.8
	20	7.0	0.1	2.40	0.06	25.6	1.0	870	20	31.3	0.9
	28	6.1	0.1	2.87	0.08	32	1	1080	30	39	1
150	7	8.7	0.1	1.09	0.03	11.1	0.3	380	10	13.7	0.4
	14	7.8	0.1	0.89	0.02	10.3	0.3	350	8	12.6	0.3
	20	8.5	0.1	1.14	0.03	11.8	0.4	400	10	14.5	0.4
	20	8.9	0.1	1.10	0.03	11.1	0.4	380	10	13.6	0.5
	47	7.0	0.3	1.34	0.03	16.1	0.7	550	10	19.7	0.5
	56	8.2	0.2	0.98	0.03	10.7	0.4	360	10	13.1	0.5

a The content of $^{152}Eu^{3+}$ in the solid is referred to the total ^{152}Eu in solid plus liquid.
b Calculated taking into account the weight of the solid and the retained amount of europium.
c This calculation corresponds to an evaluation of the mol% of silicon corresponding to $Eu_2Si_2O_7$.

Figure 1

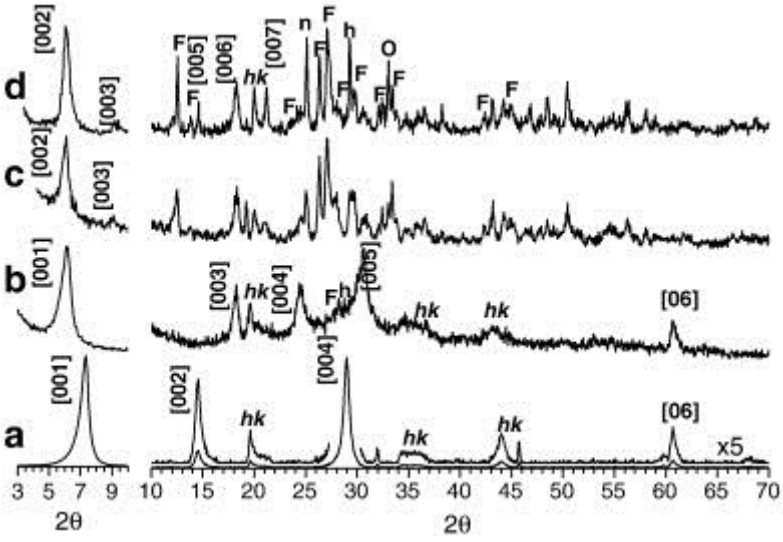
d
c
b
a
[002]
[003]
[001]
[005]
[006]
[007]
hk
n
F
h
O
[004]
[06]
x5
3 5 7 9
10 15 20 25 30 35 40 45 50 55 60 65 70
2θ
2θ

Figure 2

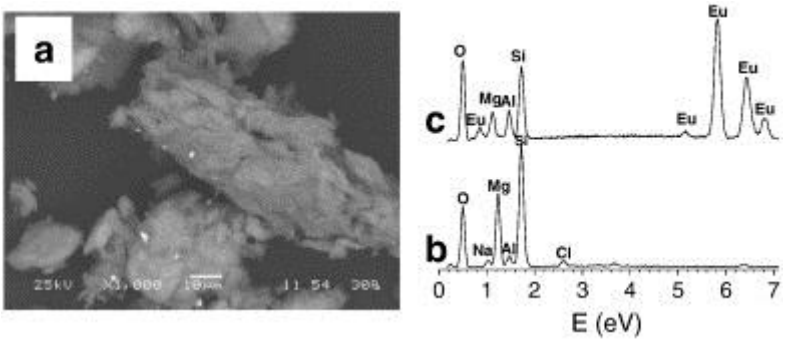

Figure 3

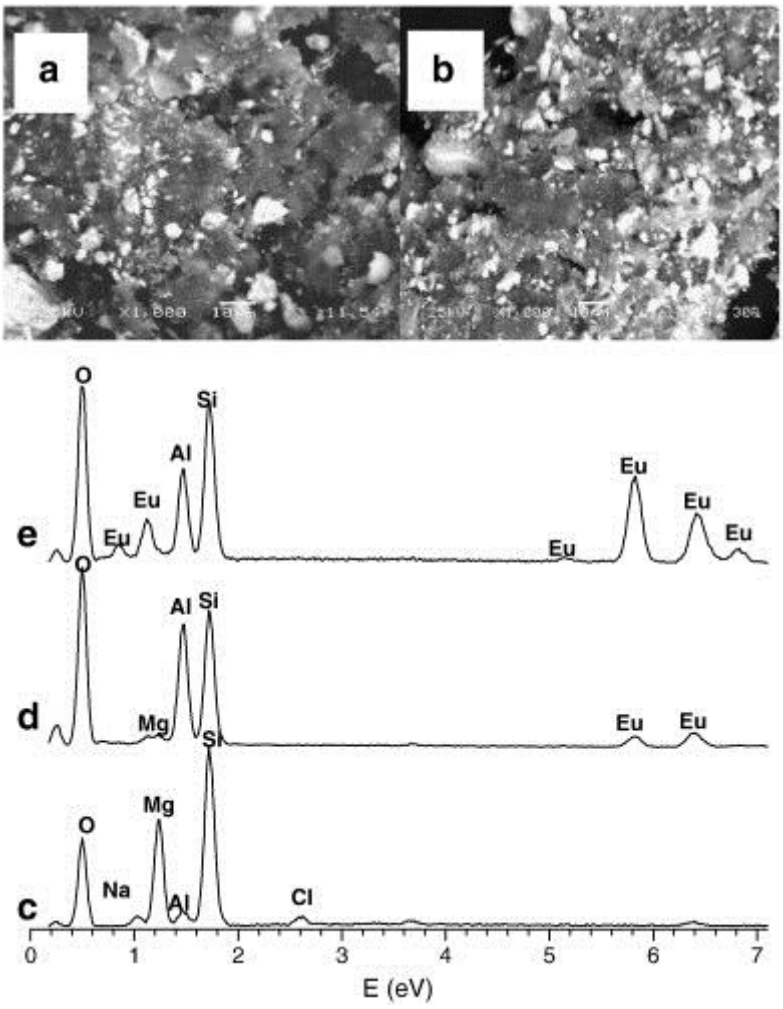
a
b
e
O
Si
Al
Eu
Eu
Eu
Eu
Eu
Eu
d
O
Al
Si
Mg
Eu
Eu
Si
c
O
Mg
Na
Al
Cl
0
1
2
3
4
5
6
7
E (eV)

Figure 4

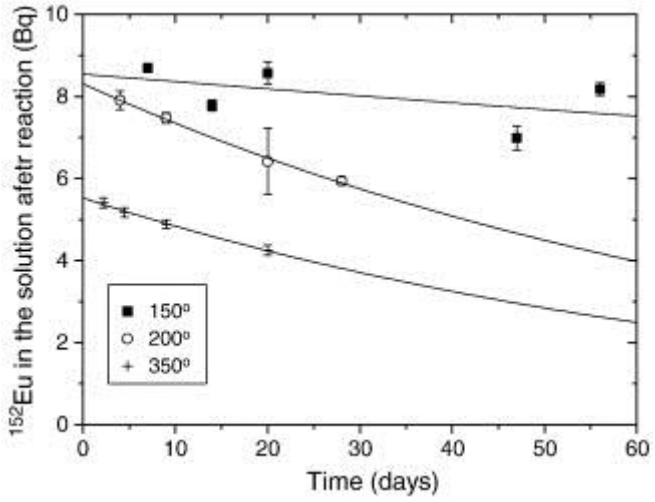
^{152}Eu in the solution afetr reaction (Bq)
Time (days)
150°
200°
350°
0
2
4
6
8
10
0
10
20
30
40
50
60